PALEOCEANOGRAPHY, VOL. 14, NO. 4, PAGES 441-456, AUGUST 1999

Orbital controls on the El Niño/Southern Oscillation and the tropical climate

A.C. Clement,[1] R. Seager, and M.A. Cane

Lamont-Doherty Earth Observatory of Columbia University, Palisades, New York

Abstract. The global synchroneity of glacial-interglacial events is one of the major problems in understanding the link between Milankovitch forcing and the climate of the late Quaternary. In this study we isolate a part of the climate system, the tropical Pacific, and test its sensitivity to changes in solar forcing associated with changes in the Earth's orbital parameters. We use a simplified coupled ocean-atmosphere model that is run for the past 150,000 years and forced with Milankovitch changes in the solar insolation. This system responds primarily to the precessional cycle in solar forcing and is capable of generating a mean response to the changes in the seasonal distribution of solar radiation even while the annual mean insolation is roughly constant. The mean response to the precessional forcing is due to an interaction between an altered seasonal cycle and the El Niño/Southern Oscillation (ENSO). Changes in the ENSO behavior result in a mean tropical climate change. The hypothesis is advanced that such a change in the tropical climate can generate a globally synchronous climate response to Milankovitch forcing.

1. Introduction

During the Quaternary, paleoclimatic records from all over the world show major events in global ice volume that happen on the same timescales as those associated with changes in the Earth's orbital parameters, the so-called Milankovitch forcing [*Crowley and North*, 1991]. In this paper we explore the link between these changes in solar insolation and the Earth's climate, focusing on the past 150 kyr. The changes in solar insolation at the top of the atmosphere associated with Milankovitch forcing are small when averaged globally and annually. This fact has led researchers to look for mechanisms that can amplify the forcing in a particular season or at a specific latitude. The most common explanation for the appearance of Milankovitch frequencies in the data involves processes occuring in the high northern latitude summer. It is argued that cool summers will lead to ice growth and initiate a number of positive feedbacks involving ocean thermohaline circulation, atmospheric circulation, and the dynamics of ice sheets [*Imbrie et al.*, 1992; *Broecker and Denton*, 1989]. These ideas, however, fail to explain the global extent of these climate events. Ice sheets and glaciers in the Southern Hemisphere are observed to decay approximately synchronously with those in the Northern Hemisphere [*Broecker and Denton, 1989; Lowell et al.*, 1995], while the change in summer insolation due to precession is out of phase between the Northern and Southern Hemispheres. Further, modeling studies with general circulation models (GCMs) fail to produce a global response to changes in the North Atlantic region [*Rind et al.*, 1986; *Manabe and Stouffer*, 1988]. Changes in the atmospheric CO_2 content are an additional possible feedback in the response of the climate to Milankovitch forcing and can provide a global response to changes in sources or sinks of CO_2. However, the mechanism by which CO_2 changes on these timescales is unclear [*Broecker*, 1995]. Furthermore, simulations of the Last Glacial Maximum (LGM) [*Broccoli and Manabe*, 1987; *Hewitt and Mitchell*, 1997] that impose the estimated drop in CO_2 fail to produce the amount of tropical cooling at the LGM that has been observed [*Guilderson et al.*, 1994; *Beck et al.*, 1997; *Stute et al.*, 1995; *Schrag et al.*, 1996; *Colinvaux et al.*, 1996]. The lack of a demonstrable effect of changes in the North Atlantic on the global climate and the insufficient cooling due to CO_2 at the LGM suggest that something is missing in our understanding of the link between global climate change and Milankovitch forcing.

Here we turn our attention to a part of the climate system that is known to be capable of organizing climate on a global scale: the tropics. Interannual variability in the tropical Pacific associated with the El Niño/Southern O scillation (ENSO) has been shown to impact climate over wide regions of the globe [*Ropelewski and Halpert*, 1987; 1989]. Modeling studies

[1]Now at the Laboratoire d'Océanographie Dynamique et de Climatologie, Université de Paris 6, Paris, France.

Paper number 1999PA900013.
0883-8305/99/1999PA900013$12.00

of past climates have not generally focussed on this region of the globe. Studies with atmospheric GCMs [e.g., *Rind et al.*, 1986; *Broccoli and Manabe*, 1987] necessarily do not account for coupled interactions, and coupled GCMs are only just beginning to include enough resolution to faithfully represent the coupled physics [*Bush and Philander*, 1998; *Hewitt and Mitchell*, 1998; D. DeWitt and E. Schneider, The tropical ocean response to a change in orbital forcing, submitted to *Journal of Climate*, 1999, hereinafter referred to as DeWitt and Schneider, submitted manuscript, 1999].

On the other hand, much understanding has been gained about the modern tropical climate by studying ENSO. At the heart of ENSO is a positive feedback between the ocean and atmosphere. A reduced equatorial SST gradient, as in the warm phase of ENSO, leads to a slackening of the trade winds, reduced equatorial upwelling, and a deepening of the thermocline in the eastern equatorial Pacific, all of which further weaken the SST gradient [*Bjerknes*, 1969; *Cane*, 1986]. In the cold phase the feedbacks push the system in the opposite direction. An increased equatorial SST gradient is enhanced by stronger trades, more equatorial upwelling, and a steeper thermocline tilt. The observational record indicates that ENSO tends to have the most power at 2-7 year periods. These interactions, however, are not restricted to this timescale. The same coupled interactions are thought to be instrumental in establishing the annual mean state of the tropical Pacific [*Dijkstra and Neelin*, 1995] as well as the seasonal cycle [*Chang*, 1996]. The observed phase locking between ENSO and the seasonal cycle [*Rasmusson and Carpenter*, 1982] implies an interaction between the interannual and seasonal timescales [*Münnich et al.*, 1991; *Tziperman et al.*, 1994; *Chang et al.*, 1994]. In short, the tropical Pacific climatology must be thought of as the result of similar physics operating on a variety of timescales that interact with each other and cannot be separated.

In this study we extend the study of ENSO-like variability to the past 150 kyr using a simplified model of the coupled ocean atmosphere system in the tropical Pacific. Model results are presented in section 2 with limitations of the model arrangement laid out in section 3. section 4 provides a summary of the late Quaternary records of eastern equatorial Pacific climate change and relates them to the model results. The potential implications of the results for the global climate are discussed in section 5, and the argument is put forth that accounting for coupled interactions in the tropics can potentially explain some aspects of the climate response to Milankovitch forcing during that last 150 kyr.

2. Modeling Experiments

We perform experiments with the Zebiak-Cane ENSO model [*Zebiak and Cane*, 1987]. This is a coupled ocean-atmosphere model of the tropical Pacific that computes anomalies in the circulation and sea surface temperature (SST) about a mean climatology that is specified from observations. The ocean model domain is 124°E to 80°W and 29°N to 29°S and has closed boundaries on all sides, while the atmosphere is global. The main dynamics in the atmosphere and ocean are described by linear shallow water equations on an equatorial beta plane. In the ocean an additional shallow frictional layer of constant depth (50 m) is included to account for the intensification of wind driven currents near the surface. The time step of the ocean model is 10 days. At each time step the ocean and atmosphere are coupled through a parameterization of the atmospheric heating. The atmospheric heating anomaly is computed from the SST anomaly, the specified background surface wind divergence field, and the modeled divergence anomaly. The atmosphere model then computes the steady state wind field anomalies from this heating, which are used to drive the ocean model. An anomalous ocean circulation and thermocline depth are computed, which are then used to compute a new SST anomaly. The subsurface temperature anomaly is parameterized as a nonlinear function of the thermocline depth anomaly. This coupled model produces self-sustained interannual oscillations and contains the main physics thought to be relevant for ENSO.

The model has an initial state with zero anomalies in all fields and is run for 150,000 years, forced with variations in solar insolation due to changes in eccentricity, obliquity, and precession of the equinoxes [*Berger*, 1978]. The solar forcing is implemented as an anomalous heat flux into the ocean surface. The top of the atmosphere solar radiation anomaly relative to today is computed as a function of time before present (Ka), season (τ), and latitude (θ), and converted to an anomalous surface heat flux by:

$$F_o'(Ka,\tau,\theta) = Q_s(T_a + 0.0019\theta_z) - F_o(0,\tau,\theta) \quad (1)$$

where $T_a = 0.7$ and is the transmissivity of the atmosphere that is meant to represent the bulk effect of absorption and reflection of solar radiation by all atmosphere constituents, Q_s is the derived solar radiation at the top of the atmosphere, θ_z is the solar zenith angle [*Berger*, 1978], and $F_o(0,\tau,\theta)$ is the modern distribution of surface solar radiation similarly computed. An unforced control run of 150,000 years is also performed with the model.

The average over 500 year nonoverlapping intervals of the NINO3 index (the SST anomaly averaged over 150°W to 90°W and 5°S to 5°N) is plotted in Figure 1a along with the anomalous solar forcing on the equator (Figure 1b). The NINO3 index is generally taken to be indicative of ENSO. The mean NINO3 value for the control run is 0.4K [*Zebiak and Cane*, 1987], which is subtracted from the NINO3 index of

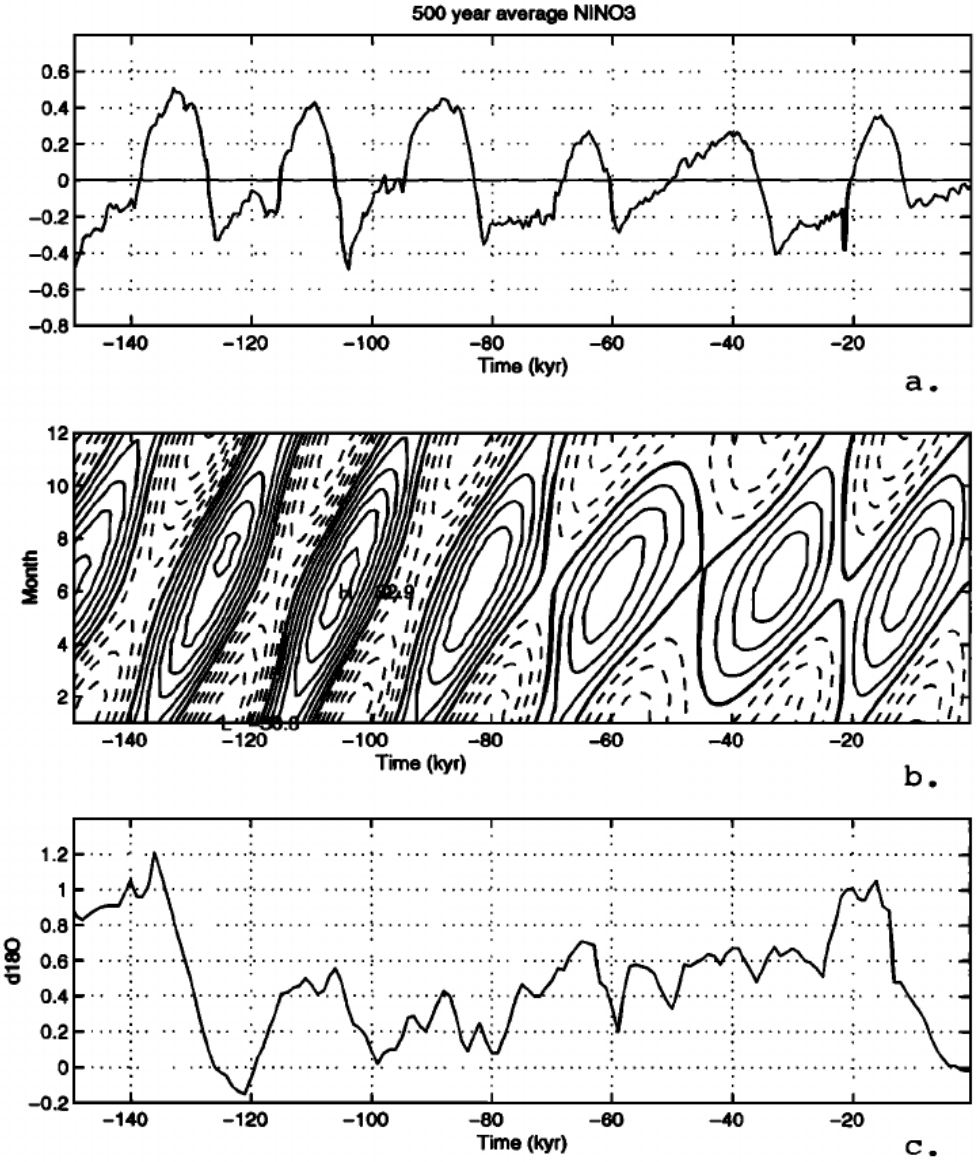

Figure 1. (a) The 500 year average NINO3 (degrees Celsius) index from Zebiak-Cane model [*Zebiak and Cane*, 1987] forced with Milankovitch solar forcing as a function of thousand years before present. (b) Contour plot of the anomalous heat flux (W m^{-2}) into the ocean surface on the equator used to force the Zebiak-Cane model as a function of time before present and month of the year. The contour interval is 5 W m^{-2} with solid lines indicating positive values and dashed lines indicating negative. (c) For reference the global ice volume curve (per mil) is plotted that shows the major glacial- interglacial stages over the past 150 kyr [from *Labeyrie et al.*, 1987]. Note that time is running from left to right so that the zero intercept of the age axis is at the right.

the forced run in all subsequent analyses. A global ice volume curve [*Labeyrie et al.*, 1987] is plotted for reference (Figure 1c). The dominant period for the late Quaternary (after 700 ka) ice volume curve is 100 kyr, which does not appear to be strong in the model experiments (though a longer run is necessary to evaluate this quantitatively). While the annual mean Milankovitch forcing in the tropics is close to zero, the index clearly shows a mean response to the precessional forcing at a period of 21 kyr, which is also apparent in the ice volume curve. In the model, there is significant power in the 11 kyr band. Power in this frequency band has been observed in some tropical records [*McIntyre and Molfino*, 1996; *Berger and Loutre*, 1997], but the 11 kyr response of this model will be investigated elsewhere. There is no response to the obliquity cycle (41 kyr) in the model. Warm periods in the model generally occur when perihelion (anomalous heating) is in January to June, and cold periods occur when perihelion is in July to December.

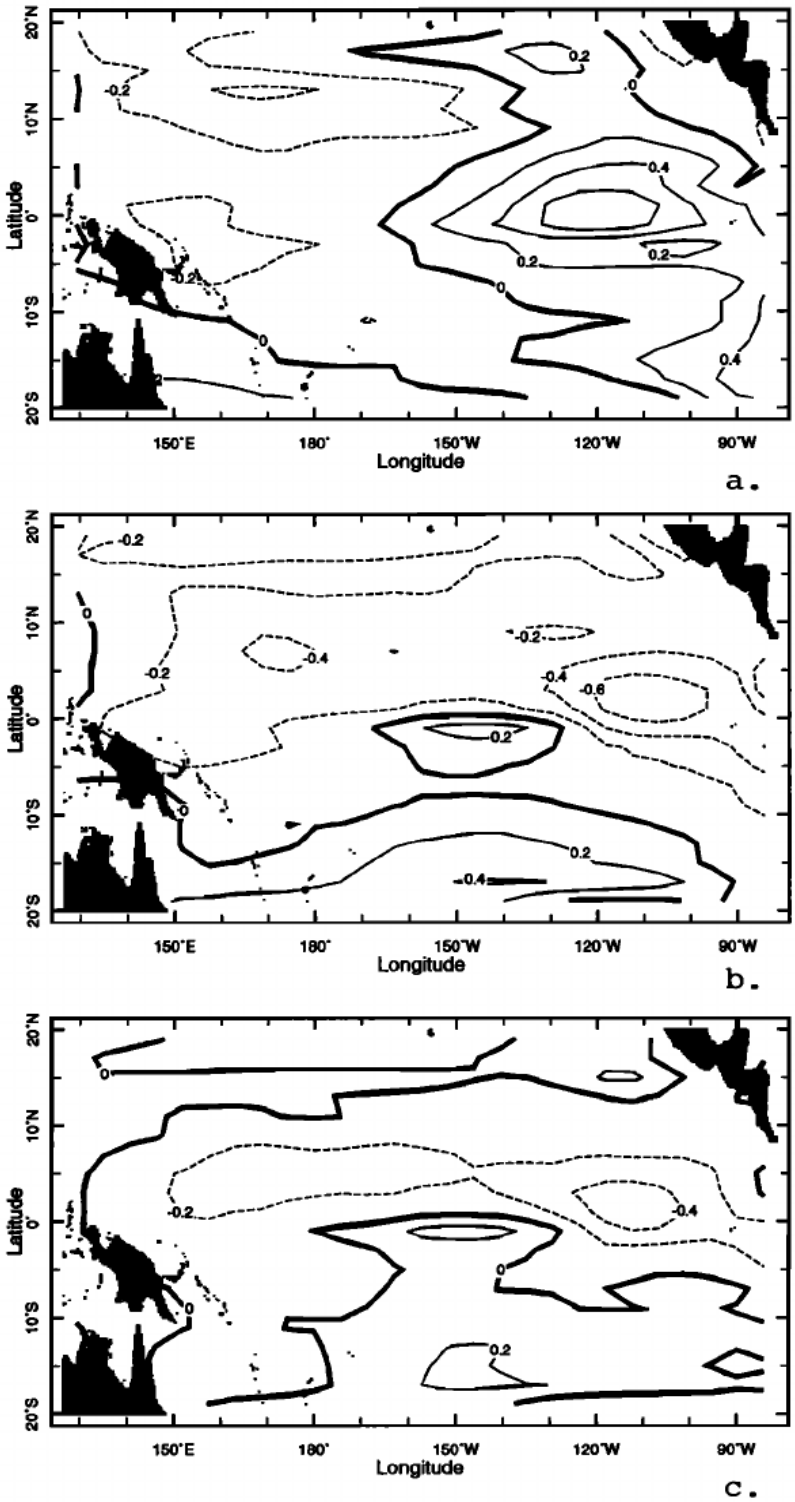

Figure 2. Average sea surface temperature (SST) anomaly in 5 kyr intervals over one precessional cycle: (a) 133-128, (b) 127-122, (c) 121-116, and (d) 115-110 kyr B.P.

The spatial structure of the long-term mean SST anomalies over one precessional cycle (Figure 2) has some of the main features of ENSO SST anomalies.

The maximum signal occurs in the eastern equatorial Pacific, and there is little signal in the off-equatorial regions. This long-term mean change in the eastern equatorial Pacific is due to a change in the ENSO variability. Figures 3a and 3b show the frequency of warm and cold ENSO events over 500 year intervals. These statistics are determined using the annual mean

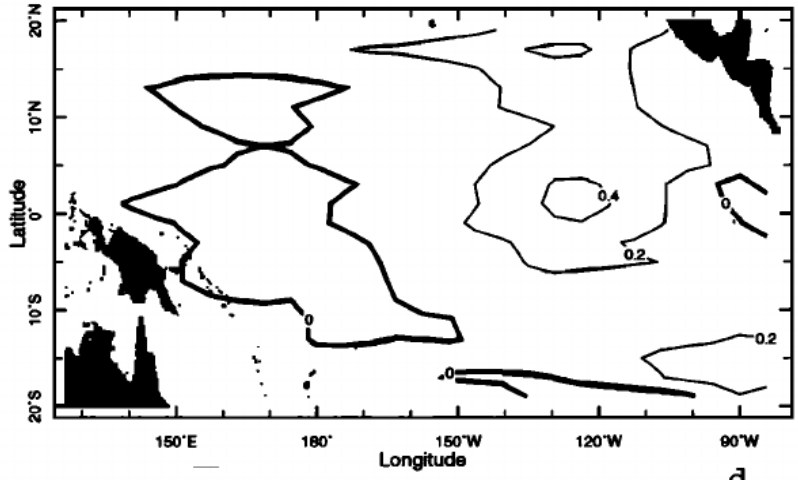

Figure 2. (continued)

NINO3 index. A warm event is defined here to occur when the annual mean NINO3 index is > 1 K, and a cold event is when the index is < -1 K. This threshold value for counting ENSO events was chosen because it conforms to the typical definition of interannual events in the literature [i.e., *Tziperman et al.*, 1994], and because anomalies of this size generally occur only on interannual timescales. The mean amplitude of events is also shown (Figure 3c). The number of warm and cold events and mean amplitude from the control run with 95% confidence limits are plotted for reference. More frequent and larger warm events occur during warm periods, while cold event frequency and amplitude are slightly larger during the cold periods.

A look at the time series and spectra shows more clearly how the character of the events change. Figure 4 shows 100 year segments from the control run NINO3 time series and from typical warm peri-

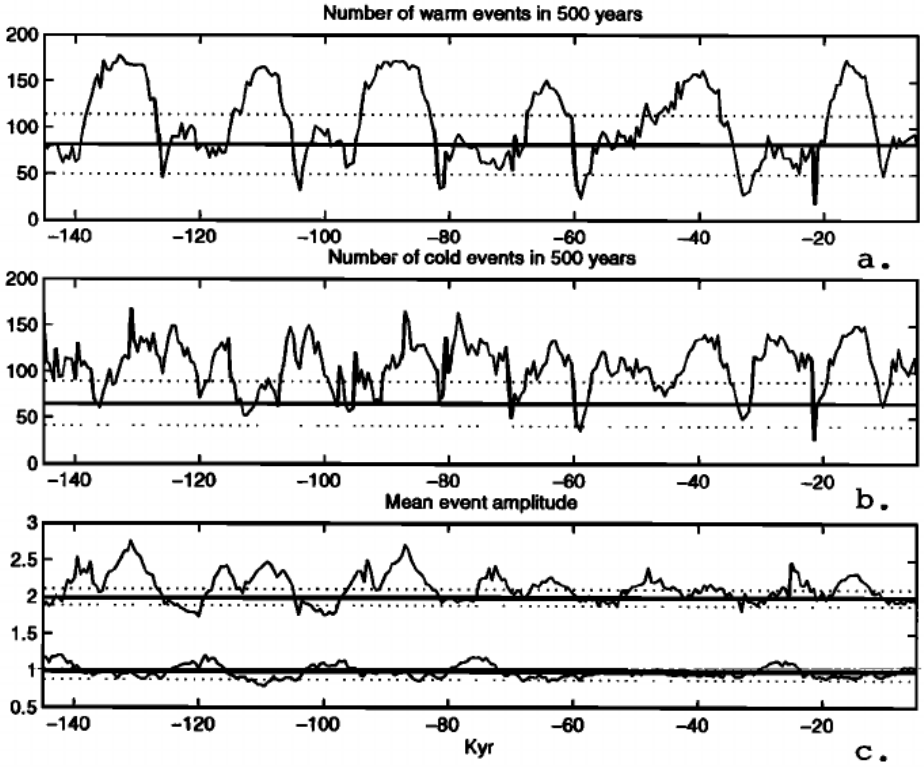

Figure 3. Statistics of events: (a) number of warm events defined as in text for 500 year nonoverlapping periods, (b) number of cold events and (c) mean amplitude of warm (upper curve) and cold (lower curve) events. Bold line shows the mean values for each of the statistics for the control run with 95% confidence limits plotted (dotted).

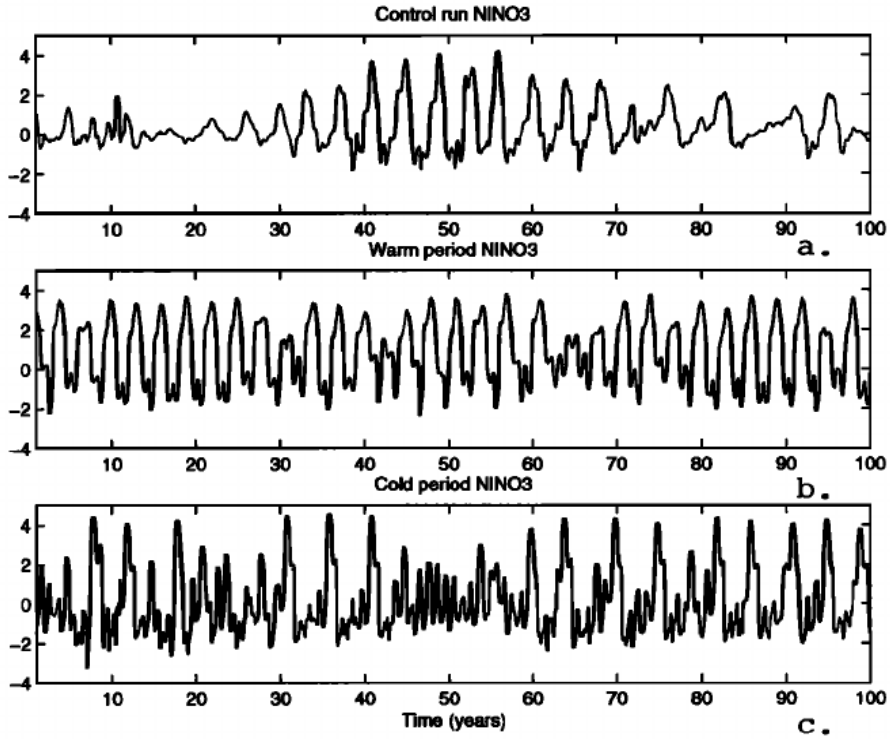

Figure 4. NINO3 time series segments from the (a) control run, (b) warm period of the forced model run (i.e., 135 ka), and (c) cold period from the forced model run (i.e., 75 ka).

ods (i.e., 135 ka) and cold periods (i.e., 75 ka). The multitaper spectrum [*Mann and Lees*, 1996, and references therein] computed for nonoverlapping 500 year segments is shown in Figure 5. In the control run the peak frequency occurs at 4 years. During the warm periods, events are larger and more regular, and the spectra shows that the peak period shifts to 3 years. During the cold periods, cold events tend to be more frequent, but the spectrum shows a less well defined peak frequency. Instead, the interannual variability is spread over a wide range of frequencies.

We wish to understand how the forcing, which is close to zero when averaged over the year, can generate a nonzero mean response. Supposing that the model responds more strongly to the forcing in one season so that the mean will be primarily determined by the forcing in that season, we perform experiments in which the forcing occurs during only 3 months of the year, with zero forcing the rest of the year. Twelve experiments are performed varying the months during which the forcing occurs with January indicating forcing from December through February, etc. Figure 6 shows the NINO3 response to this 3 month forcing for a 20 W m^{-2} heating (lower solid line) and a 20 W m^{-2} cooling (upper solid line) as a function of the month of the forcing. The model response is clearly largest in the latter half of the year, with a maximum when the forcing is centered in July. A cooling at that time tends to produce a warm NINO3 anomaly and vice versa.

The cause of the seasonally varying sensitivity to the forcing lies in the seasonal cycle of the mean divergence on the equator. This is illustrated schematically in Figure 7. We consider a uniform heating of the tropical Pacific, which approximates the precessional forcing. When a uniform forcing is applied, it will initially generate a uniform SST anomaly that will affect the atmosphere differently in different seasons. For example, in spring (April in Figure 7) the Intertropical Convergence Zone (ITCZ) is near the equator, and the wind field is convergent all across the equator. Thus the uniform SST anomaly will generate a more or less zonally symmetric response in atmospheric heating. However, in late summer/early fall (October in Figure 7) the eastern Pacific ITCZ moves north, and the wind field becomes divergent in the east while remaining convergent in the west. Thus the warming of the tropical ocean yields a larger heating of the atmosphere in the western Pacific, where the mean (background) wind field is already convergent, than in the eastern Pacific, where the strong mean divergence suppresses the development of deep convection. The zonal asymmetry in atmospheric heating anomaly drives easterly wind anomalies at the equator. The coupled system amplifies this perturbation on an interannual timescale via

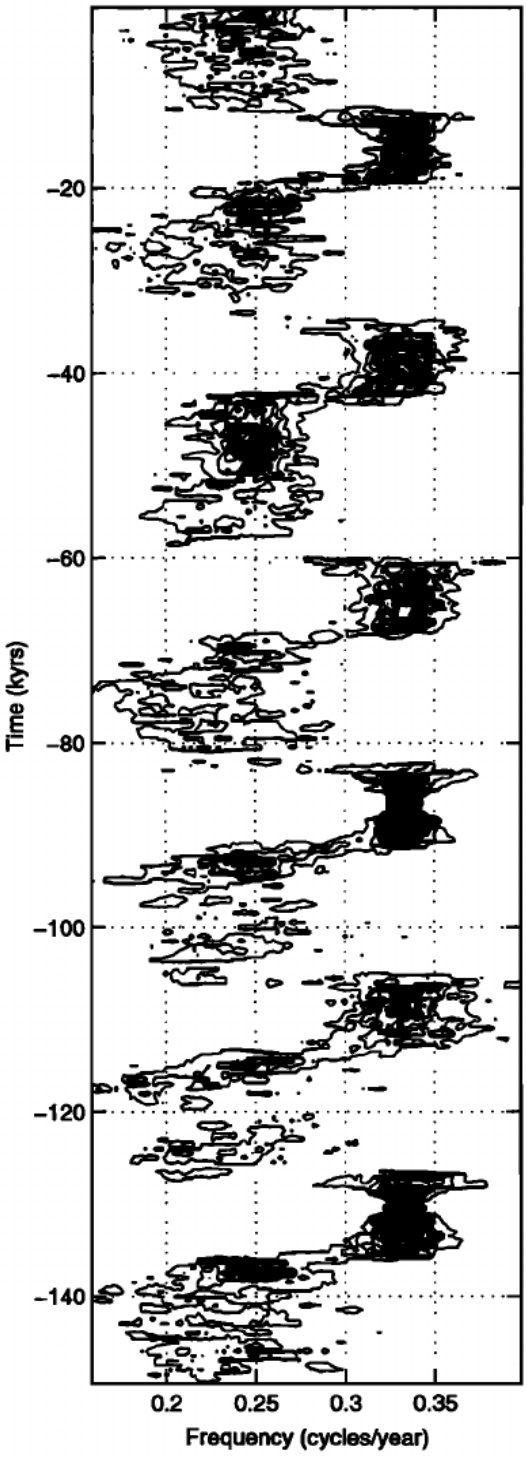

Figure 5. Contour plot of the multitaper spectrum of the NINO3 time series computed each 500 years.

the same unstable interactions that give rise to ENSO, and the result is a cooler east Pacific or more La Niña-like conditions. A uniform cooling yields the opposite response: little or no response to the forcing in spring, while in the late summer/early fall the result is westerlies on the equator that can develop into a more El Niño-like response.

Thus the background seasonal cycle in the wind divergence field is responsible for converting the zonally uniform solar forcing into a zonally asymmetric response most efficiently in the late summer/early fall. This important point can be demonstrated by removing the seasonal cycle in the background wind divergence field. If we replace the monthly divergence field with that for March and perform the same 12 experiments, the seasonal cycle in the response of NINO3 is entirely removed (Figure 6, dashed lines).

The range of ENSO behavior demonstrated here has been documented previously in this model [*Tziperman et al.*, 1994; 1997] as well as in similar models [*Chang et al.*, 1994]. In those studies, various alterations to the seasonal cycle were made that shifted the peak frequency of ENSO and also in some cases damped out the interannual variability entirely. This behavior was due to nonlinear interactions between the seasonal cycle and the interannual variability that entrain the dominant frequency into various resonances of the system. The model responds in a similar way to the Milankovitch forcing. If coupled dynamics did not play a role, then the SST would simply warm and cool uniformly over the basin following the forcing with some time delay, and the mean change over the year would vanish. Instead, coupled interactions alter the response to the zonally uniform forcing to give a more zonally asymmetric response in the late summer/early fall. The system is most poised to amplify this initial response in summer because this is the season during which conditions are most favorable for the rapid growth of both positive and negative anomalies because of an effective increase in coupling strength in that season [*Zebiak and Cane*, 1987]. In short, the system responds to Milankovitch forcing on both the seasonal and interannual timescales, and the nonlinear interaction between these timescales yields a change in the ENSO variability that results in a mean tropical climate change. This change is dictated primarily by the forcing in the late summer, with warming in the summer giving a La Niña-like response and cooling in the summer giving an El Niño-like response.

It should be noted that the changes in the NINO3 index (Figure 1a), the statistics of the events (Figure 3a,b), and the spectra (Figure 5) do not vary smoothly in time, nor do they appear to follow the solar forcing exactly. There also appears to be a change in the coherence of the number of warm and cold events at 70 ka after which the amplitude of the seasonal cycle in solar forcing is diminished (Figure 1b). This behavior can be attributed to, or taken as evidence of, the nonlinearity of this system. While we have identified the gross behavior of the model in response to the Milankovitch forcing, there are details of the response that remain to be explained.

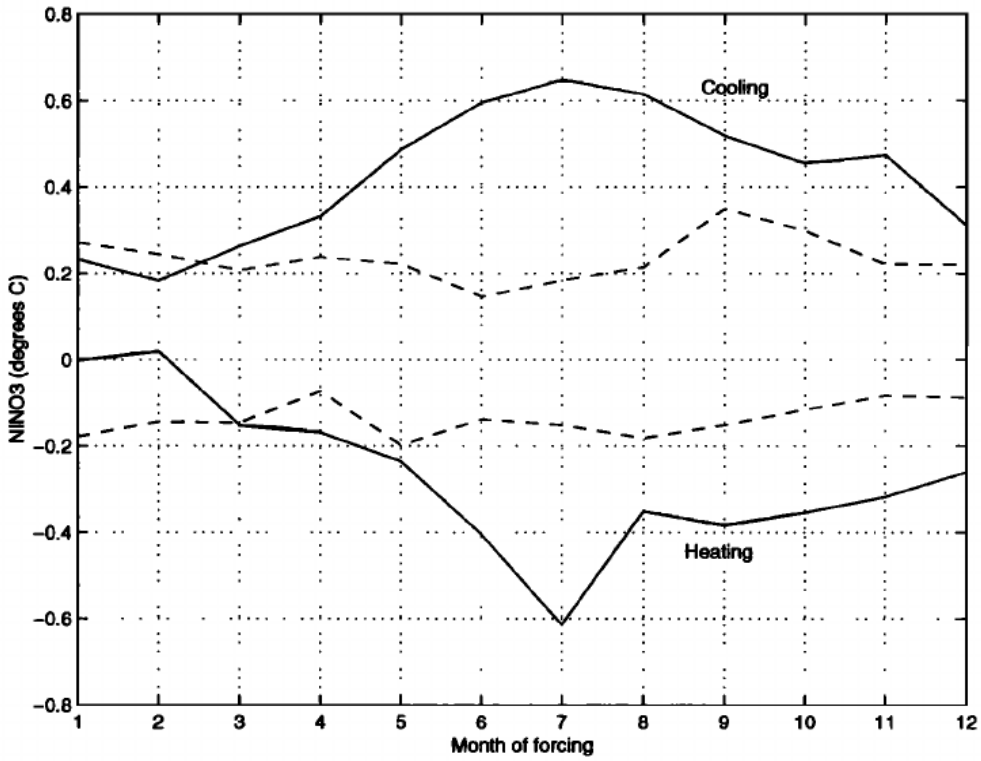

Figure 6. NINO3 response to a 3 month forcing centered on the month of the axis. For example, 2 corresponds to a forcing in January, February and March. The upper solid line is the response to a cooling, and the lower solid line is the response to a warming. The dashed lines show the results when the background wind divergence field is held at its March values.

3. Limitations of the Model Arrangement

While this model is highly simplified, it has the convenient property that we know a great deal about its limitations. It is an anomaly model and need not conserve energy. Since the annual mean forcing averaged over the basin is close to zero, the anomaly surface heat flux should also be close to zero when averaged over the basin and the year if energy is conserved. However, the imbalance over the long run amounts to a net ocean heat flux of less than 2 W m^{-2} which is the order of the annual and basin mean net surface heat flux associated with the Milankovitch forcing. This imbalance amounts to an approximately 0.1 K temperature anomaly, which is considerably smaller than the response of the model to precession.

While energy conservation does not appear to be a serious issue for the present study, the specification of the background climatology about which the components of the model are linearized is problematic. The fixed background state probably ties the tropical climatology too tightly to the modern climate. In particular, it is likely that the seasonal position of the ITCZ will change as the climate changes and significantly alter the seasonal cycle, but the model will restrict the extent to which this can happen. In addition, the equatorial vertical thermal structure specified in the model has a significant impact on the interannual variability [*Zebiak*, 1984]. It is not clear how this will change as the climate changes. The temperature and sources of the equatorial thermocline water are issues that are currently under investigation [*Liu et al.*, 1994; *Lu and McCreary*, 1995; *Fine et al.*, 1987; *Rodgers et al.*, 1999]. Generally, it is believed that there are about equal amounts of Southern and Northern Hemisphere water in the equatorial thermocline. If this is the case, it can be argued that the temperature of the upwelled water should not change much on precessional timescales. Consider the simple picture that the equatorial thermocline is ventilated from the northern subtropics during March (Northern Hemisphere spring) when the mixed layer is deepest, and from the south in September (Southern Hemisphere spring). Since the precessional cycle is out of phase between the equinoxes, when the northern subtropics are being cooled in March, the southern subtropics are being warmed in September. Thus we expect the contributions to cooling or warming of the equatorial thermocline from the southern and northern subtropical source waters to at least partially cancel on this timescale in the presence of adequate cross-isopycnal motion in the equatorial thermocline. However, much more needs to

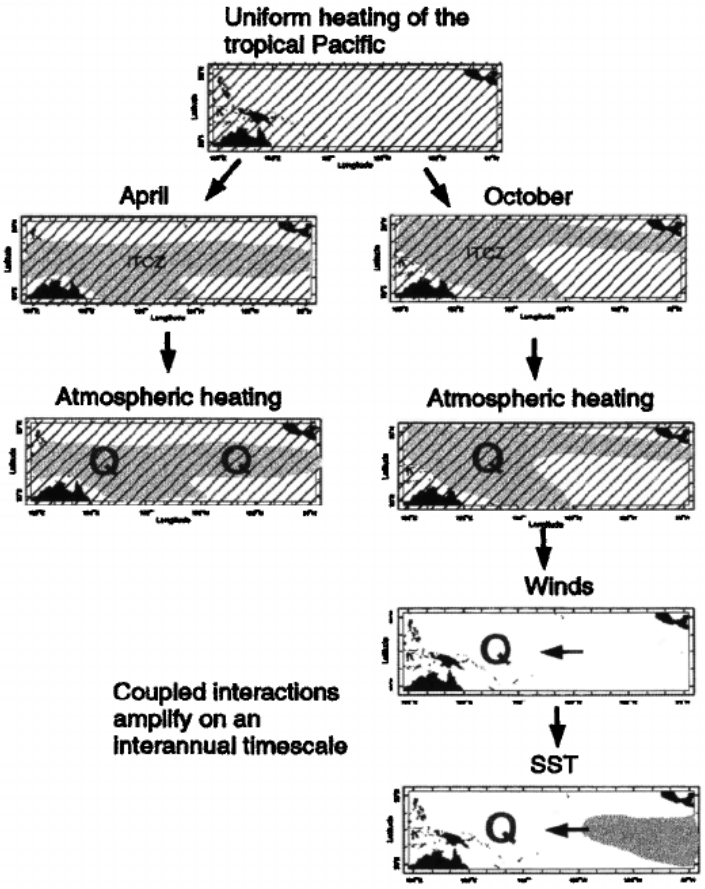

Figure 7. Schematic representation of the mechanism by which the tropical Pacific coupled ocean-atmosphere system responds to Milankovitch forcing. We consider (top) a uniform heating of the tropical Pacific ocean (cross-hatching represents a heating or warm SST anomaly). The seasonal position (April or October) of the Intertropical Convergence Zone (ITCZ)- the region of mean wind field convergence, high precipitation, or atmospheric heating, is represented by the shaded region. In April the total effect of the warm SST anomaly and the background wind field convergence gives an atmospheric heating that is uniform across the equator and hence will not be amplified by zonally asymmetric coupled interactions. On the other hand, in October, when the ITCZ is north of the equator in the eastern Pacific, the combined effect of the SST anomaly and the background wind field convergence gives a zonally asymmetric atmospheric heating that drives easterly winds. The coupled system amplifies this signal on an interannual timescale. The result is a (bottom) La Ninã-like SST anomaly (shaded region).

be understood about the connection between climate and the structure of the equatorial thermocline.

The phase of the mean seasonal cycle, essential to the model's response to precessional forcing, is also specified in the background state. The mean change in NINO3 is related to the sign of the forcing in late summer/fall when the divergence field is most zonally asymmetric and the growth of perturbations is the largest. If the changes in seasonal cycle substantially went beyond what the model can simulate, it is not clear how the precessional forcing would affect the ENSO variability since it originates in the nonlinear interactions between the seasonal cycle and the wave dynamics [*Zebiak and Cane*, 1987; *Tziperman et al.*, 1994; 1997; *Chang et al.*, 1994]. However, recent investigations of the factors controlling the phase of the seasonal cycle in the eastern equatorial Pacific generally point to the continental configuration and heating over land [*Philander et al.*, 1996]. DeWitt and Schneider, submitted manuscript, 1999] performed a coupled GCM experiment changing the phase of the precessional cycle opposite to today's. While the seasonal cycle in the eastern equatorial Pacific is slightly shifted relative to today, the phasing is approximately the same with warming in the first half of the year and cooling in the latter half. Thus, it is possible that the phase of the seasonal cycle remained unchanged during the late Quaternary when the continental configuration was approximately the same as in the present day.

A more serious caveat concerns the simplicity of the

atmosphere model. In this model, atmospheric heating drives the low level wind field, but, otherwise the atmosphere only damps the SST anomalies. This does not account for the numerous atmospheric feedbacks that have been demonstrated to play a role in the determination of tropical SST. The role of atmospheric convective boundary layer processes [*Sarachik*, 1978; *Betts and Ridgway*, 1989], atmospheric circulation [*Wallace*, 1992; *Fu et al.*, 1990; *Hartmann and Michelsen*, 1993; *Pierrehumbert*, 1995], ocean circulation [*Clement and Seager*, 1999], stratus clouds [*Miller*, 1997], and tropospheric water vapor content [*Larson and Hartmann*, 1999, R. Seager et al., Glacial cooling in the tropics: Exploring the roles of tropospheric water vapor, surface wind speed and boundary layer processes submitted to *Journal of Atmospheric Sciences*, 1999, hereinafter referred to as Seager et al., submitted manuscript, 1999] have all been been suggested as having the potential to greatly influence the tropical SST, although the interaction between all of these factors has not been clearly laid out. It remains to be seen whether these atmospheric processes would enhance, damp, or alter the response of the model to Milankovitch forcing.

The Zebiak-Cane model does not include active land surfaces. Changes in the heating over land associated with the Milankovitch forcing are capable of moving and changing the strength of the atmospheric convection. For example, there are considerable atmospheric modeling efforts underway to determine the response of the African and Indian monsoon to the change in solar forcing at 6 ka [*Joussaume et al.*, 1999]. Coupled GCMs have shown that ocean-atmosphere interactions can play a role in the response of these monsoon systems to solar forcing [*Kutzbach and Liu*, 1997; *Hewitt and Mitchell*, 1998] In the modern climate, changes in the equatorial Pacific SST gradient are somewhat correlated with changes in the strength of the Asian monsoon [*Shukla and Paolina*, 1983]. The monsoon tends to be stronger during a La Niña (increased equatorial SST gradient) and weaker during an El Niño. The model produces a La Niña-like response when there is anomalous solar heating in the late summer/early fall. This configuration of solar forcing would also tend to enhance the monsoon. The stronger monsoon and a more La Niña-like state could reinforce each other, presenting a potential positive feedback that is absent in our simple model. A more complete model is necessary to investigate coupled ocean-atmosphere-land interactions in response to Milankovitch forcing.

One further limitation of the model is the lack of the extratropics. While changes in the extratropical climate will no doubt have an impact on the tropics, the focus for this study is on the possibility that changes in the tropical climate can drive changes at higher latitudes. For this reason it is in the interest of this study to fix the climate of the extratropics. The interaction of the tropics and extratropics will be the subject of future work.

These caveats raise the possibility that the mechanism presented here for a tropical Pacific response to precessional forcing may be altered or overwhelmed by other processes in the climate system. We turn now to the paleoclimate record to see if there is any indication of this kind of mechanism operating in the tropical Pacific during the late Quaternary.

4. Paleoclimatic Data From the Eastern Equatorial Pacific

Our model results predict a strong response to precessional forcing in the eastern equatorial Pacific for the period between 150 ka and the present. High-resolution data from this region are rather sparse because of low sedimentation rates, but we attempt to summarize what is thought to be the precessional response in the eastern equatorial Pacific for the Pliocene-Pleistocene. A study of Pliocene-Pleistocene variability from selected sites in the eastern equatorial Pacific shows that Milankovitch periods appeared in the δ^{18}O of planktonic species only after 3.2 Ma [*Cannariato and Ravelo*, 1997]. This coincides with the closing of the Panama seaway, a shoaling of the thermocline in the east, and the establishment of the modern SST gradient across the Pacific [*Chaisson*, 1995]. *Cannariato and Ravelo* [1997, p. 805] suggested that the "hydrographic response to Milankovitch forcing is enhanced by air-sea interactions which maintain the relatively steep Pleistocene trans-Pacific gradients." Later in the Pleistocene (from 1 Ma to present), the planktonic δ^{18}O from the eastern equatorial Pacific show 100, 41 and 23 kyr periods, which are coherent with benthic δ^{18}O from the same region, but the relative power in these frequency bands varies over time [*Ravelo and Shackleton*, 1995; *Pisias and Rea* 1988] as well as spatially [*Hagelberg et al.*, 1995]. *Lyle et al.* [1992] showed an in-phase relation between an SST proxy and the precessional component of insolation in cores from the central equatorial Pacific. Productivity proxies from the tropical Atlantic and Pacific [*Lyle*, 1988] and the equatorial Indian [*Beaufort et al.*, 1997] show strong precessional signals that lead the ice-volume signal.

Ravelo and Shackleton [1995] have constructed an oceanic record from Ocean Drilling Program (ODP) site 851 (2°45′N, 110°35′W) that can be compared more immediately with the model results. They create a thermocline depth proxy by subtracting the δ^{18}O of mixed-layer dwelling *Globigerinoides sacculifer* from the δ^{18}O of a species living at the bas e of the photic zone (*Globorotalia tumida*) and one that lives within the thermocline (*Neogloboquadrina duterei*). Taking the difference removes the global ice volume effect on δ^{18}O. When the δ^{18}O values of the mixed layer dwellers and the

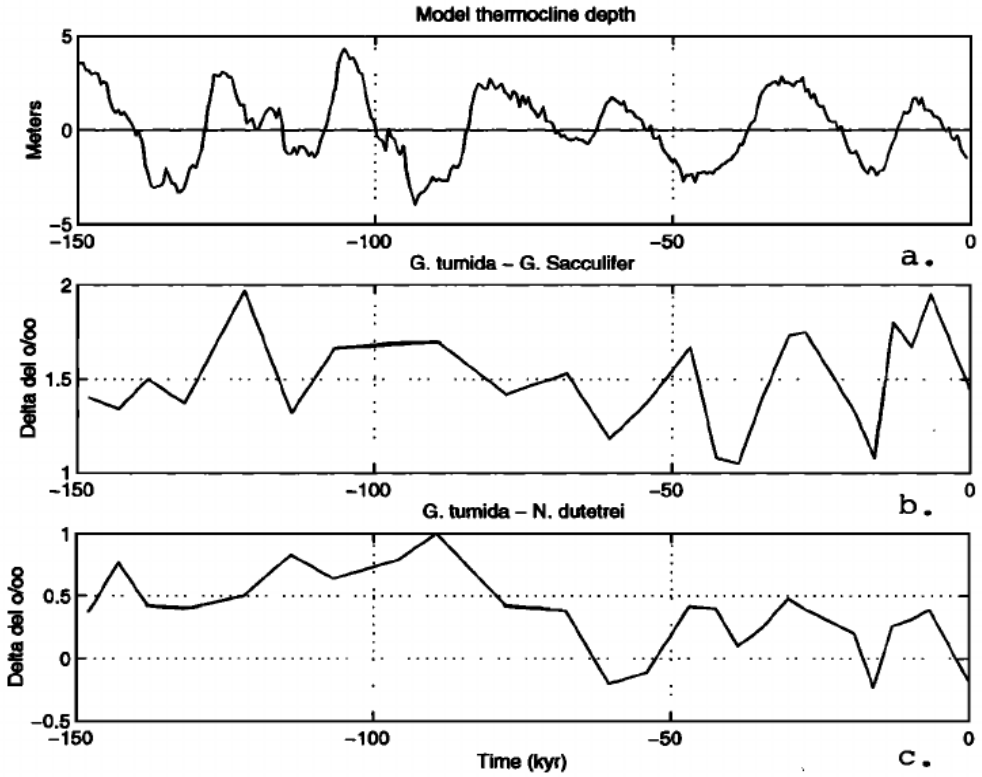

Figure 8. (a) The 500 year average upper layer depth anomaly in the model run at 110 °W 2°N (meters). Negative values indicate a deeper thermocline; positive values indicate a shallower thermocline. (b) *Globorotalia tumida- Globigerinoides sacculifer* $\Delta\delta^{18}$O *o/oo.* (c) *G. tumida - Neogloboquadrina duterei* $\Delta\delta^{18}$O *o/oo* from *Ravelo and Shackleton* [1995].

species from lower in the water column are similar, they are interpreted as a deepening of the thermocline, and as the difference gets large, the values are taken to indicate a shoaling of the thermocline. Glacial-interglacial changes in SST may also affect the thermocline proxy as it affects the δ^{18}O of *G. sacculifer.* To account for this, *Ravelo and Shackleton* [1995] compare *G. tumida-G. sacculifer* to *G. tumida-N. duterei* and find that they are coherent only at about the 19 kyr period. Thus the thermocline variability they found at this site is only in the precessional band. However, this thermocline proxy does not appear to show a significant precessional response before 700 ka [*Cannariato and Ravelo*, 1997].

The model thermocline anomalies at 2°N and 110°W and the two thermocline proxies from site 851 (*G. tumida-G. sacculifer* and *G. tumida-N. dutertrei*) are compared in Figure 8. Negative values for the model thermocline indicate a deeper thermocline that goes with periods of increased El Niños and a warmer mean NINO3 index. Smaller values for the $\Delta\delta^{18}$O indicate a deeper thermocline. While the proxy records and the model results do not match perfectly, there is some correspondence. The resolution of the record is only 5 kyr, which makes the comparison somewhat difficult for this timescale. Considering the numerous caveats listed in section 3, we do not expect the model to be able to predict all low-frequency excursions of the equatorial thermocline in the real world. However, the dominance of the precessional frequencies in the model and proxy and the phase relationship between them suggest that the mechanism outlined here could have had some impact on the equatorial thermocline in the late Quaternary.

Records of atmospheric methane trapped in ice cores [*Chappellaz et al.*, 1993; *Brook et al.*, 1996] show the 100, 41, and 20 kyr Milankovitch periods, but the precessional band is larger than in the other climate proxies of the ice cores. *Chappellaz et al.* [1993] have argued that these changes in atmospheric methane reflect mainly changes in the tropical climate rather than high latitudes. The tropical climate change predicted by the model has the potential for changing the tropical sources of methane. For example, an increased frequency of El Niños would tend to shift the convective systems away from the Indonesian land masses and cause drying there. ENSO has also been shown to affect other parts of the tropics, causing changing patterns of drought through atmospheric teleconnections. While there are likely to be other factors that affect the tropical methane sources (i.e., sea level change and

monsoons), it is possible that changes in the interannual variability in response to precessional forcing may alter the hydrological cycle in a way that is recorded in the methane of the ice cores.

Changes in ENSO behavior have previously been invoked to explain some climate proxies from the eastern equatorial Pacific. *Sandweiss et al.* [1996] infer from mollusk fauna at archaeological sites on the Peruvian coast that between 8 and 5 ka there was a continuous presence of warm waters offshore. They speculated that this may reflect a permanent El Niño-like state, though this interpretation has been challenged by *DeVries et al.* [1997] and *Wells and Noller* [1997]. *Colinvaux* [1972] showed that the Galapagos Islands had become gradually wetter since 10 ka, with the largest premodern lake levels occuring between 6 and 8 ka. This may be interpreted as a warmer eastern equatorial Pacific SST at that time which would be roughly consistent with the *Sandweiss et al.* [1996] results. The Zebiak-Cane model results for this time period, however, suggest more La Niña-like conditions, and Ravelo and Shackelton's thermocline depth proxy from site 851 indicates a shallower thermocline at that time. Other oceanic proxies give mixed signals. In particular, proxies for productivity from the coastal eastern equatorial Pacific show enhanced productivity/upwelling or a shallower thermocline [*Farrell et al.*, 1995] which is inconsistent with a permanent El Niño state. It is likely that ENSO-like climate change does not capture the full range of tropical climate variability on Milankovitch timescales. However, the records are as yet too sparse to resolve the large-scale pattern.

5. Discussion

We have demonstrated a mechanism, closely related to ENSO, by which the tropical Pacific coupled system can amplify Milankovitch forcing. Numerous past works have investigated the range of variability of the ENSO system by exploring the sensitivity to model parameters and the strength of the annual cycle [see *Neelin et al.* 1998]. These works have demonstrated the complexity of the coupled dynamics with the system exhibiting a variety of timescales and resonances that can be excited through nonlinear interactions. The present study extends this work to the response of the ENSO system to a real climate forcing, the Milankovitch forcing. We show that the seasonally varying forcing with close to zero annual mean associated with the precession of the equinoxes can push the system into different climate regimes where the character of ENSO is significantly altered. A warm mean state occurs when there is anomalous cooling in the late summer/fall, and a cold mean state occurs when there is anomalous warming in those seasons. The initially uniform cooling is translated seasonally into a spatial structure that the coupled interactions in the system can amplify on an interannual timescale, thus changing the statistics of the ENSO events.

Changes in the behavior of ENSO in the model result in a mean tropical climate change. A demonstration of the likelihood of forced, or natural, ENSO-like climate change on longer than interannual timescales comes from the modern climate record. In studies of the modern climate that attempt to separate interannual and decadal variability and trends in the tropical Pacific SST the ENSO pattern, or something quite similar, emerges [*Zhang et al.*, 1997; *Latif et al.*, 1997; *Cane et al.*, 1997]. The simplest explanation for this is that coupled interactions can operate on any timescale, possibly generating decadal variability on their own [i.e., *Zebiak and Cane*, 1991], responding to forcing from the extra-tropics on a longer timescale (R. Kleeman et al., A mechanism for generating ENSO decadal variability, submitted to *Science*, 1999), or responding to forcing external to the climate system, such as anthropogenic greenhouse gases [*Cane et al.*, 1997; A. Timmerman et al., ENSO response to greenhouse warming, submitted to *Geophysical Research Letters*, 1999]. Thus tropical climate change must be thought of as the net result of coupled dynamics operating on different timescales that interact with each other and that are difficult to separate. Perhaps a more useful idea, suggested by *Palmer* [1993], is that climate change in a nonlinear system with strong attractors will manifest as a change in the probability that the system will reside in a particular regime without changing the character of the attractors. The primary mode of variability in the tropical climate is ENSO. The spatial structure of this mode of variability is unaltered by the solar forcing (in the Cane-Zebiak model at least). Rather, the Milankovitch forcing changes the temporal evolution which results in a mean tropical climate change because of a change in the statistics of events. This provides a more general way of understanding forced climate change in a system where nonlinear interactions are important.

In this model study many aspects of the climate system are not accounted for that could affect the results presented here. To test this mechanism in the presence of more complete climate physics, it is necessary to perform similar experiments with a model that computes its own mean state and seasonal cycle (i.e., a coupled GCM). In such a model it should be possible to see how the tropical Pacific is affected by changes in the monsoons, adjustment of the vertical thermal structure of the tropical ocean, and by the processes thought to have an affect on tropical SST (i.e., stratus clouds, ocean and atmospheric circulation and atmospheric water vapor content). It is difficult to speculate about how all these processes will interact with each other and with ENSO. Some studies of the response of the tropical Pacific to precessional changes in the solar forcing have already been performed with coupled GCMs [e.g., DeWitt and Schneider, submitted manuscript, 1999]. In

that experiment the amplitude and frequency of ENSO did not change, though there is a change in the timing of events. In the current generation of coupled GCMs, however, ENSO variability tends to be fairly weak, and there is reason to believe that the mechanisms of the real ENSO are not fully captured by these models [see *Delecluse et al.*, 1998]. Experiments with other coupled GCMs are necessary to test the robustness of the response of ENSO to Milankovitch forcing.

Ultimately, these ideas must be tested against paleoclimate data from the tropical Pacific. ENSO-like climate change will tend to have the largest signal in the central and eastern equatorial Pacific. The data from from this region are sparse and, at certain times in the past (i.e., 8-5 ka), inconclusive. In general, more spatial coverage is needed to determine the large-scale patterns of SST, productivity, or thermocline depth change at certain times during the late Quaternary. For this, a temporal resolution of the order of 1000 years should be sufficient to explore the response of the tropical Pacific to Milankovitch forcing. In addition, studies such as that of *Andreason and Ravelo* [1997], where the thermocline structure at the LGM was reconstructed over much of the tropical Pacific basin using foraminiferal assemblages, would also be useful for other time slices. Another potentially useful data set comes from fossil corals [see *Cole et al.*, 1992]. These records have the advantage of high temporal resolution and semiquantitative SST measurements, which are possible through multiple proxies (e.g. O^{18}, Sr/Ca). The difficulties lie in sample replication, diagenetic alteration of older samples, and the interpretation of low-frequency variability (e.g., decadal, centennial, and secular). If the spatial pattern of ENSO-related SST anomalies was similar to that observed today, the largest signal is to be expected in the central and eastern equatorial Pacific, but other sites in the tropical Pacific may sufficiently record ENSO variability of the past [see *Evans et al.*, 1998]. From various fossil coral records around the tropical Pacific and Indian Oceans, it may be possible to estimate the range of ENSO behavior and to test whether there is some connection between ENSO and Milankovitch forcing.

Here we advance the hypothesis that ENSO-like climate change can generate a globally synchronous response to Milankovitch forcing. In order to affect the global mean temperature, changes in the tropics must initiate feedbacks that alter the energy budget of the planet. This could result from either a change in the global planetary albedo or through changes in the greenhouse effect such that the planet emits to space at the same effective radiating temperature but with a different surface temperature. The most likely candidates of effecting such changes are ice sheets, clouds, water vapor, and CO_2. However, none of these is likely to change without some change in atmospheric circulation.

The changes in the tropical climate demonstrated here have the potential for altering the global atmospheric circulation, which would impact both the Northern and Southern Hemispheres. For example, ENSO alters the strength of the local and zonal mean Hadley circulation [*Chou*, 1994; *Oort and Yienger*, 1996; *Soden*, 1997; *Sun and Trenberth*, 1998]. *Lindzen and Pan* [1994] have suggested that poleward transports of heat and moisture can be affected by the strength of the Hadley cell [see also *Hou 1998*], and lead to conditions that can favor ice build up and decay. Also, *Kukla and Gavin* [1992] have also pointed out that changes in the mean tropical climate may affect the supply of moisture to the high latitudes, which could lead to ice growth.

The zonally asymmetric circulation is equally important. On interannual timescales, changes in the tropical climate have been demonstrated to affect climate over much of the globe through changes in the stationary wave patterns [*Trenberth et al.*, 1998]. Generally, these teleconnections have been attributed to changes in the location of tropical convection, which in turn affect the midlatitude circulation. In our experiments, east-west shifts in the mean position of the convecting regions occur as a result of changes in the relative likelihood of warm and cold events. The effects of ENSO can be large in North America, where ice sheets grow [*Cane*, 1998]. Could changes in ENSO result in altered stationary wave patterns that would favor ice build up or decay in this region?

Furthermore, Seager et al. [submitted manuscript, 1999] have shown that changes in tropical tropospheric water vapor can have an appreciable effect on the mean tropical SST. Changes in water vapor can result from changes in the the cloud microphysics that determine the precipitation efficiency of the convective towers, but the strength and sign of this feedback is poorly known. They suggest that an increase in the strength of the Hadley cell has a net drying effect on the tropical troposphere. It is possible that changes in ENSO will affect the strength of the Hadley cell and the other components of the atmospheric circulation, thereby altering the tropical tropospheric humidity and initiating a potentially important climate feedback.

Changes in low cloud cover are also potentially important agents of climate change. *Klein and Hartmann* [1993] noted a correlation between subtropical stratus cloud amount and ENSO with increased cloud cover during the cold phase. Stratus clouds have a large net climate forcing; an increase in stratus cloud amount should cool the planet and hence appears to be a potential positive feedback on ENSO timescales. On the other hand, *Miller* [1997] and *Clement and Seager* [1999] have suggested that low-level stratus would be a negative feedback on climate change.

In summary, the mechanism demonstrated here for

the response of the tropical climate to Milankovitch forcing could have an effect on any number of these processes in the climate system with a possible impact on the global energy budget. This raises the possibility that rather than being a passive player, the tropics can drive globally synchronous climate change on Milankovitch timescales. This is, without a doubt, not the whole story. As the high latitude climate changes, the tropical system would be affected either through the ocean [e.g., *Bush and Philander*, 1998] or atmosphere [A. Broccoli, Extratropical influences on tropical paleoclimates submitted to *AGU Monograph: Mechanisms of millennial scale global climate change*, 1999]. The link between the tropics and high latitudes on these timescales must be further explored. This study opens up some new possibilities for understanding global climate change on Milankovitch timescales, but answers will require investigations using more complete models of the tropical climate system and further data from the tropics.

Acknowledgments. The authors would like to thank S. Zebiak for his continual supply of helpful insight. The comments of C. Ravelo, J. Lynch-Steiglitz, D. Schrag, J. McManus, D. Oppo, M. Elliot, M. Evans, T. Koutavas and B. Linsley all helped to educate us about the paleoclimate record. We also thank the three reviewers of this paper for their helpful comments. A. Clement and R. Seager were supported by NASA grant NAGW-916. RS received additional support from NOAA grant UCSIO-10775411D/NA47GP0188 (The Consortium on the Oceans Role in Climate). MAC was supported by NOAA grant NA36GP0074-02.

References

Andreason, D. J., and A. C. Ravelo, Tropical Pacific Ocean thermocline depth reconstructions for the Last Glacial Maximum, *Paleoceanography*, *12*, 395–413, 1997.

Beaufort, L., Y. Lancelot, P. Camberlin, O. Cayre, E. Vincent, F. Bassinot, and L. Labeyrie, Insolation cycles as a major control of equatorial Indian ocean primary production, *Science*, *278*, 1451–1454, 1997.

Beck, J., J. Récy, F. Taylor, R. L. Edwards, and G. Cabioch, Abrupt changes in the early Holocene tropical sea surface temperature derived from coral records, *Nature*, *385*, 705–707, 1997.

Berger, A., Long-term variations of daily insolation and Quaternary climate changes, *J. Atmos. Sci.*, *35*, 2362–2367, 1978.

Berger, A., and M. Loutre, Intertropical latitudes and precessional and half-precessional cycles, *Science*, *278*, 1476–1478, 1997.

Betts, A. K., and W. Ridgway, Climatic equilibrium of the atmospheric convective boundary layer over a tropical ocean, *J. Atmos. Sci.*, *46*, 2621–2641, 1989.

Bjerknes, J., Atmospheric teleconnections from the equatorial Pacific, *Mon. Weather. Rev.*, *97*, 163–172, 1969.

Broccoli, A., and S. Manabe, The influence of continental ice, atmospheric CO_2 and land albedo on the climate of the Last Glacial Maximum, *Clim. Dyn.*, *1*, 87–99, 1987.

Broecker, W., *The Glacial World According to Wally*, 318 pp., Lamont-Doherty Earth Observatory, Palisades, NY., 1995.

Broecker, W., and G. Denton, The role of ocean-atmosphere reorganizations in glacial cycles, *Geochim. et Cosmochim. Acta*, *53*, 2465–2501, 1989.

Brook, E., T. Sowers, and J. Orchardo, Rapid variations in atmospheric methane concentration during the past 110,000 years, *Science*, *273*, 1087–1091, 1996.

Bush, A.B.G., and S.G.H. Philander, The role of ocean-atmosphere interactions in tropical cooling during the last glacial maximum, *Science*, *279*, 1341–1344, 1998.

Cane, M., El Niño, *Annu. Rev. Earth Planet Sci.*, *14*, 43–70, 1986.

Cane, M. A., Climate change: A role for the tropical Pacific, *Science*, *282*, 59–61, 1998.

Cane, M. A., A. C. Clement, A. Kaplan, Y. Kushnir, D. Pozdnyakov, R. Seager, S. E. Zebiak, and R. Murtugudde, Twentieth century sea surface tempature trends, *Science*, *275*, 957–906, 1997.

Cannariato, K., and A. Ravelo, Plio-Pleistocene evolution of eastern tropical Pacific surface water circulation and thermocline depth, *Paleoceanography*, *12*, 805–820, 1997.

Chaisson, W., Planktonic formaniferal populations and paleooceanographic change in the tropical Pacific: A comparison of west (leg 130) and east (leg 138), latest Miocene to Pleistocene , *Proc. Ocean Drill. Program Sci. Res.*, *138*, 555–597, 1995.

Chang, P., The role of the dynamic ocean-atmosphere interactions in the tropical seasonal cycle, *J. Clim.*, *9*, 2973–2985, 1996.

Chang, P., B. Wang, T. Li, and L. Ji, Interactions between the seasonal cycle and the Southern Oscillation: Frequency entrainment and chaos in a coupled ocean-atmosphere model, *Geophys. Res. Lett.*, *21*, 2817–2820, 1994.

Chappellaz, J., T. Blunier, D. Raynaud, J. Barnola, J. Schwander, and B. Stauffer, Synchronous changes in atmospheric CH_4 and Greenland climate between 40 and 8 kyr BP, *Nature*, *366*, 443–445, 1993.

Chou, M.-D., Coolness in the tropical Pacific during an El Niño episode, *J. Clim.*, *7*, 1684–1692, 1994.

Clement, A. C., and R. Seager, Climate and the tropical oceans, *J. Clim.*, 1999, in press.

Cole, J., G. Shen, R. Fairbanks, and M. Moore, Coral monitors of El Niño/Southern Oscillation dynamics across the equatorial Pacific, in *El Niño: Historical and paleoclimatic aspects of the Southern Oscillation*, edited by E. by H.F. Diaz and V. Margraf, pp. 349–375, Cambridge Univ. Press, New York, 1992.

Colinvaux, P., Climate and the Galapagos Islands, *Nature*, *240*, 17–20, 1972.

Colinvaux, P., P. D. Oliveira, J. Moreno, M. Miller, and M. Bush, A long pollen record from lowland Amazonia: Forest and cooling in glacial times, *Science*, *274*, 85–88, 1996.

Crowley, T., and G. North, *Paleoclimatology* , Oxford Univ. Press, New York., 1991.

Delecluse, P., M. Davey, Y. Kitamura, S. Philander, M. Suarez, and L. Bengtsson, Coupled general circulation modeling of the tropical Pacific, *J. Geophys. Res.*, *103*, 14,357–14,373, 1998.

DeVries, T. J., L. Ortlieb, and A. Diaz, Determining the early history of ENSO, *Science*, *276*, 965–966, 1997.

Dijkstra, H. A., and J. D. Neelin, Ocean-atmosphere interaction and the tropical climatology, II, Why the Pacific cold tongue is in the east, *J. Clim.*, *8*, 1343–1359, 1995.

Evans, M., A. Kaplan, and M. Cane, Optimal sites for coral-based reconstruction of global sea surface temperature, *Paleoceanography*, *13*, 502–516, 1998.

Farrell, J., T. Pedersen, S. Calvert, and

B. Nielsen, Glacial-interglacial changes in the equatorial Pacific Ocean, *Nature*, *377*, 514–517, 1995.

Fine, R., W. H. Peterson, and H. G. Ostlund, The penetration of Tritium into the tropical Pacific, *J. Phys. Oceanog.*, *5*, 553–564, 1987.

Fu, R., A. D. DelGenio, and W. B. Rossow, Behavior of deep convective clouds in the tropical Pacific deduced from ISCCP radiances, *J. Clim.*, *3*, 1129–1152, 1990.

Guilderson, T. P., R. G. Fairbanks, and J. L. Rubenstone, Tropical temperature variations since 20 000 years ago: Modulating interhemispheric climate change, *Science*, *263*, 663–665, 1994.

Hagelberg, T., N. Pisias, L. Mayer, N. Shackleton, and A. Mix, Spatial and temporal variability of the late Neogene equatorial carbonate: Leg 138, *Proc. Ocean Drill. Program Sci. Res.*, *138*, 321–336, 1995.

Hartmann, D. L., and M. Michelsen, Large scale effects on the regulation of tropical sea surface temperature, *J. Clim.*, *6*, 2049–2062, 1993.

Hewitt, C. D., and J. F. B. Mitchell, Radiative forcing and response of a GCM to ice age boundary conditions: cloud feedback and climate sensitivity, *Clim. Dyn.*, *13*, 821–834, 1997.

Hewitt, C. D., and J. F. B. Mitchell, A fully coupled GCM simulation of the climate of the mid-Holocene, *Geophys. Res. Lett.*, *25*, 361–364, 1998.

Hou, A., Hadley circulation as a modulator of the extratropical climate, *J. Atmos. Sci.*, *55*, 2437–2457, 1998.

Imbrie, J., J. Hays, D. Martinson, A. McIntyre, A. Mix, A. Morley, N. Pisias, W. Prell, and N. Shackleton, The orbital theory of Pleistocene climate: Support from a revised chronology of the marine $\delta^{18}O$ record, in *Milankovich and Climate, Vol. I*, edited by A. L. Berger et al., pp. 269–305, D. Reidel, Hingham, MA, 1984.

Imbrie, J. I., et al., On the stucture and origin of major glaciation cycles, 1, Linear responses to Milankovitch forcing, *Paleoceanography*, *7*, 701–738, 1992.

Joussaume, S., et al., Monsoon changes for 6000 years ago: Results of 18 simulations from the Paleoclimate Modeling Intercomparison Project (PMIP), *Geophys. Res. Lett.*, 1999, in press.

Klein, S. A., and D. L. Hartmann, The seasonal cycle of low stratiform clouds, *J. Clim.*, *6*, 1587–1606, 1993.

Kukla, G., and J. Gavin, Insolation regime of the warm to cold transitions, in *NATO Advanced Research Institute: Start of a Glacier*, edited by G. Kukla and E. Went, pp. 307–339, Lab. Oceanogr. Phys. du Museum Nat. Hist. Nat. Paris, Paris, France, 1992.

Kutzbach, J., and Z. Liu, Response of the African monsoon to orbital forcing and ocean feedbacks in the middle Holocene, *Science*, *278*, 440–443, 1997.

Labeyrie, L., J. Duplessy, and P. Blanc, Variations in mode of formation and temperature of oceanic deep waters over the past 125,000 years, *Nature*, *327*, 477–482, 1987.

Larson, K., and D. L. Hartmann, A two box equilibrium model of the tropics, *J. Clim.*, 1999, in press.

Latif, M., R. Kleeman, and C. Eckert, Greenhouse warming, decadal variability or El Niño? An attempt to understand the anomalous 1990s, *J. Clim.*, *10*, 2221–2239, 1997.

Lindzen, R. S., and W. Pan, A note on orbital control of equator-pole heat fluxes, *Clim. Dyn.*, *10*, 49–57, 1994.

Liu, Z., S. G. H. Philander, and R. C. Pacanowski, A GCM study of tropical-subtropical upper-ocean water exchange, *J. Phys. Oceanogr.*, *24*, 2606–2623, 1994.

Lowell, T., C. Heusser, B. Anderson, P. Moreno, A. Hauser, L. Heusser, C. Schluchter, D. Marchant, and G. Denton, Interhemispheric correlation of late Pleistocene glacial events, *Science*, *269*, 1541–1549, 1995.

Lu, P., and J. P. McCreary, Influence of the ITCZ on the flow of thermocline water from the subtropical to the equatorial ocean, *J. Phys. Oceanogr.*, *25*, 3076–3088, 1995.

Lyle, M., Climatically forced organic carbon burial in equatorial Atlantic and Pacific oceans, *Nature*, *335*, 529–532, 1988.

Lyle, M. W., F. Prahl, and M. Sparrow, Upwelling and productivity changes inferred from a temperature record in the central and equatorial Pacific, *Nature*, *355*, 812–815, 1992.

Manabe, S., and R. Stouffer, Two stable equilibria of a coupled ocean-atmosphere model, *J. Clim.*, *1*, 841–866, 1988.

Mann, M., and J. Lees, Robust estimation of background noise and signal detection in climatic time series, *Clim. Change*, *33*, 409–445, 1996.

McIntyre, A., and B. Molfino, Forcing of Atlantic equatorial and subpolar millenial cycles by precession, *Science*, *274*, 1867–1870, 1996.

Miller, R. L., Tropical thermostats and low cloud cover, *J. Clim.*, *10*, 409–440, 1997.

Münnich, M., M. A. Cane, and S. E. Zebiak, A study of self-excited oscillations of the tropical ocean atmosphere system, II, Nonlinear cases., *J. Atmos. Sci.*, *48*, 1238–1248, 1991.

Neelin, J. D., D. Battisti, A. Hirst, F. Jin, Y. Wakata, T. Ymamgata, and S. Zebiak, ENSO theory, *J. Geophys. Res.*, *103*, 14,261–14,290, 1998.

Oort, A., and J. Yienger, Variability in the Hadley ciculation and its connection to ENSO, *J. Clim.*, *9*, 2751–2767, 1996.

Palmer, T. N., Extended-range atmospheric prediction and the Lorenz model, *Bull. Am. Meteorol. Soc.*, *74*, 49–65, 1993.

Philander, S., D. Gu, D. Halpern, N. Lau, T. Li, and R. Pacanowski, Why the ITCZ is mostly north of the equator, *J. Clim.*, *9*, 2958–2972, 1996.

Pierrehumbert, R. T., Thermostats, radiator fins, and the runaway greenhouse, *J. Atmos. Sci.*, *52*, 1784–1806, 1995.

Pisias, N., and D. Rea, Late Pleistocene paleoclimatology of the central equatorial Pacific: Sea surface response to the southeast trade winds, *Paleoceanography*, *3*, 21–37, 1988.

Rasmusson, E., and T. Carpenter, Variations in tropical sea surface temperature and surface wind fields associated with the Southern Oscillation/El Niño, *Mon. Weather. Rev.*, *110*, 354–384, 1982.

Ravelo, A., and N. Shackleton, Evidence for surface-water circulation changes at site 851 in the eastern equatorial Pacific Ocean., 1995.

Rind, D., D. Peteet, W. Broecker, A. McIntyre, and W. R. Ruddiman, The impact of cold North Atlantic sea surface temperature on climate: Implication for Younger Dryas cooling (11-10 k), *Clim. Dyn.*, *1*, 3–33, 1986.

Rodgers, K., M. A. Cane, N. Naik, and D. Schrag, The role of the Indonesian throughflow in equatorial Pacific thermocline ventilation , *J. Geophys. Res.*, 1999, in press.

Ropelewski, C. F., and M. S. Halpert, Global and regional scale precipitation patterns associated with the El Niño/Southern Oscillation., *Mon. Weather. Rev.*, *114*, 2352–2362, 1987.

Ropelewski, C. F., and M. S. Halpert, Precipitation patterns associated with the high index phase of the Southern Oscillation, *J. Clim.*, *2*, 268–284, 1989.

Sandweiss, D., J. Richardson, E. Reitz, H. Rollins, and K. Maasch, Geoarchaeological evidence from Peru for a 5000 year B.P. onset of El Niño, *Science*, *273*, 1531–1533, 1996.

Sarachik, E. S., Tropical sea surface temperature: An interactive one-dimensional model., *Dyn. Atmos. Oceans*, *2*, 455–469, 1978.

Schrag, D., G. Hampt, and D. Murray, Pore fluid constraints on the temperature and oxygen isotopic composition of the glacial ocean, *Science*, *272*, 1930–1931, 1996.

Shukla, J., and D. Paolina, The Southern Oscillation and long range forecasting of the summer monsoon rainfall over India, *Mon. Weather. Rev.*, *111*, 1830–1837, 1983.

Soden, B. J., Variations in the tropical greenhouse effect during El Niño, *J. Clim.*, *10*, 1050–1055, 1997.

Stute, M., M. Forster, H. Frischkorn, A. Serejo, J. Clark, P. Schlosser, W. Broecker, and G. Bonani, Cool-

ing of tropical Brazil during the Last Glacial Maximum, *Science*, *269*, 379–383, 1995.

Sun, D.-Z., and K. Trenberth, Coordinated heat removal from the equatorial Pacific during the 1986-87 El Niño, *Geophys.Res Lett.*, *25*, 2659–2662, 1998.

Trenberth, K., G. Branstator, D. Karoly, A. Kumar, N.-C. Lau, and C. Ropelewski, Progress during TOGA in understanding and modeling global teleconnections associated with tropical sea surface temperatures, *J. Geophys. Res.*, *103*, 14,291–14,324, 1998.

Tziperman, E., M. A. Cane, and S. E. Zebiak, Irregularity and locking to the seasonal cycle in an ENSO prediction model as explained by the quasi-periodicity route to chaos, *J. Atmos. Sci.*, *52*, 293–306, 1994.

Tziperman, E., S. E. Zebiak, and M. Cane, Mechanisms of seasonal-ENSO interaction, *J. Atmos. Sci.*, *54*, 61–71, 1997.

Wallace, J. M., Effect of deep convection on the regulation of tropical sea surface temperature, *Nature*, *957*, 230–231, 1992.

Wells, L. E., and J. S. Noller, Determining the early history of ENSO, *Science*, *276*, 966–966, 1997.

Zebiak, S. E., *Tropical atmosphere-ocean interaction interaction and the El Niño/Southern Oscillation phenomenon.*, Ph.D. thesis, Mass. Inst. of Technol., Cambridge, 1984.

Zebiak, S. E., and M. A. Cane, A model El Niño-Southern Oscillation, *Mon. Weather. Rev.*, *115*, 2262–2278, 1987.

Zebiak, S. E., and M. A. Cane, Natural climate variability in a coupled model., in *Greenhouse-Gas-Induced Climate Change: A Critical Appraisal of Simulations and Observations*, edited by M. E. Schlesinger, pp. 457–469, Elsevier, New York, 1991.

Zhang, Y., J. M. Wallace, and D. S. Battisti, ENSO-like decade-to-century scale variability: 1900-93, *J. Clim.*, *10*, 1004–1020, 1997.

M. Cane and R. Seager, Lamont-Doherty Earth Observatory, Palisades, NY 10964 (rich@rosie.ldeo.columbia.edu; mcane@ldeo.columbia.edu)

A. Clement, LODYC, Tour 26, étage 4, CASE100, 4 Place Jussieu, 75252 Paris, Cedex 05, France. (Amy.Clement@ipsl.jussieu.fr)

(Received October 8, 1998;
revised February 19, 1999;
accepted February 26, 1999.)